Letter

Stabilization of Asymmetric Underactuated Ships With Full-State Constraints: From Underactuated to Nonholonomic Configuration

Zhongcai Zhang, Linran Tian, Heng Su, and Yuqiang Wu

Dear Editor,

This letter addresses the stabilization control of an asymmetric underactuated surface ship with full-state constraints. To simplify the design of controller, the original ship model is transformed into a nonlinear cascade system with a minimum phase. Then, the stabilization of the cascade system is further processed into an equivalent stabilization of a reduced-order nonholonomic-like system. A discontinuous stabilization control method is proposed through a combination of state-scaling and state-dependent function transformations, nonlinear filters, and switching technologies. Stability analysis demonstrates that under the newly designed stabilization controller, the closed-loop system states are bounded and the desired state constraints are not violated.

Underactuated surface vessel (USV) plays an important role in marine operations, such as transportation, patrolling, and underwater detection [1]. Due to the lack of a controller in sway direction, the control design for USV poses a challenge to control engineering. Research on USV can be roughly divided into the stabilization and tracking control for symmetric USV [2] and asymmetric USV (including USV with stochastic disturbances) [3], [4]. The smooth time-varying control method [5] and discontinuous control method [6] are the two most commonly used methods to achieve the stabilization of USV. And Lyapunov's direct method [2], [7] and line-of-sight-based method [8] are the most effective weapons to handle tracking issues. Additionally, some simpler control strategies have also been put forward, such as cascade control methods [3], [5]. Other control issues include fixed-time-based [9] fault diagnosis control [10], etc.

Since it is difficult to directly develop a controller for USV by using traditional nonlinear control methods, the main control method is to change the USV model into a backstepping design form. However, this form is not strictly upper-triangular, which makes the design process tedious and difficult. On the other hand, it is well-known that underactuated systems and nonholonomic systems are generally studied separately, and the control relationship between them has never really examined.

This paper studies the stabilization of an asymmetric underactuated ship with full-state constraints. The main model transformation contribution is that we transform the stabilization problem of the asymmetric USV into that of an equivalent reduced-order system, and transform the equivalent reduced-order system into a nonholonomic-like system, and finally realize the transformation from system underactuated structure to nonholonomic structure. It is a new and simper way to study USV control than the existing methods, such as Lyapunov's direct approach. The main control design contribution is that we have developed a discontinuous stabilization control algorithm by using σ-scaling, state-dependent function (SDF) transformations, Barrier Lyapunov functions (BLFs), and filters, such that the resulting closed-loop system is ultimately bounded and the desired state constraints are not violated in the entire control process.

Corresponding author: Yuqiang Wu.

Citation: Z. C. Zhang, L. R. Tian, H. Su, and Y. Q. Wu, "Stabilization of asymmetric underactuated ships with full-state constraints: From underactuated to nonholonomic configuration," *IEEE/CAA J. Autom. Sinica*, vol. 9, no. 12, pp. 2197–2199, Dec. 2022.

The authors are with School of Engineering, Qufu Normal University, Rizhao 276826, China (e-mail: zhangzhongcai68@126.com; qfnutlr1999@163.com; qfnush1998@126.com; wyq@qfnu.edu.cn).

Color versions of one or more of the figures in this paper are available online at http://ieeexplore.ieee.org.

Digital Object Identifier 10.1109/JAS.2022.105848

Problem formulation: The dynamic model of the considered underactuated surface ship is expressed as [1]

$$\begin{cases}\dot{\boldsymbol{\eta}} = \mathbf{J}(\psi)\mathbf{v}\\ \mathbf{M}\dot{\mathbf{v}} = -\mathbf{C}(\mathbf{v})\mathbf{v} - \mathbf{D}\mathbf{v} + \boldsymbol{\tau}^*\end{cases}\tag{1}$$

with $\boldsymbol{\eta} = (x, y, \psi)^T$, $\mathbf{v} = (u, v, r)^T$, $\boldsymbol{\tau}^* = (\tau_u^*, 0, \tau_r^*)^T$, $\mathbf{J}(\psi) = [\cos(\psi)\ -\sin(\psi)\ 0; \sin(\psi)\ \cos(\psi)\ 0; 0\ 0\ 1]$, $\mathbf{M} = [m_{11}\ 0\ 0; 0\ m_{22}\ m_{23}; 0\ m_{32}\ m_{33}]$, $\mathbf{C} = [0\ 0\ c_{13}; 0\ 0\ c_{23}; -c_{13}\ -c_{23}\ 0]$, $\mathbf{D} = [d_{11}\ 0\ 0; 0\ d_{22}\ d_{23}; 0\ d_{32}\ d_{33}]$, $c_{13} = -m_{22}v - 0.5(m_{23} + m_{32})r$, and $c_{23} = m_{11}u$. Please see [5] for more details about this ship model.

The control objective is described as: design control inputs τ_u^* and τ_r^* such that $\lim_{t\to\infty} x(t) = 0$, $\lim_{t\to\infty} y(t) = 0$, $\lim_{t\to\infty} \psi(t) = 0$, $\lim_{t\to\infty} u(t) = 0$, $\lim_{t\to\infty} v(t) = 0$, $\lim_{t\to\infty} r(t) = 0$ as far as possible and $|x(t)| < k_x$, $|y(t)| < k_y$, $|\psi(t)| < k_\psi$, $|u(t)| < k_u$, $|v(t)| < k_v$, $|r(t)| < k_r$ where k_x, k_y, k_ψ, k_u, k_v, k_r are positive constants.

In order to convert the studied ship model into a cascade form, we first introduce the following input transformations [3]:

$$\bar{\tau}_u^* = \frac{1}{m_{11}}\tau_u^* + \Delta_1, \quad \bar{\tau}_r^* = \frac{m_{22}}{m_{22}m_{33} - m_{23}m_{32}}\tau_r^* + \Delta_2 \tag{2}$$

where $\Delta_1 = 1/(m_{11})[r(m_{22}v + 0.5(m_{23} + m_{32})r) - d_{11}u]$ and $\Delta_2 = (1/(m_{22}m_{33} - m_{23}m_{32}))[(m_{11}m_{22} - m_{22}^2)uv + (m_{32}d_{22} - m_{22}d_{32})v + (m_{32}\times d_{23} - m_{22}d_{33})r + (m_{11}m_{32} - 0.5m_{22}(m_{23} + m_{32}))ur]$. Under which, one can get that

$$\begin{cases}\dot{u} = \bar{\tau}_u^*, \quad \dot{r} = \bar{\tau}_r^*\\ \dot{v} = \dfrac{1}{m_{22}}(-m_{23}\bar{\tau}_r^* - m_{11}ur - d_{22}v - d_{23}r).\end{cases}\tag{3}$$

Next, motivated by [11], we introduce the state transformations as

$$\begin{cases}x_1 = [x + \varepsilon^*(\cos(\psi) - 1)]\cos(\psi) + (y + \varepsilon^*\sin(\psi))\sin(\psi)\\ x_2 = -[x + \varepsilon^*(\cos(\psi) - 1)]\sin(\psi) + \dfrac{1}{\beta}(v + \varepsilon^* r) - \dfrac{\gamma}{\beta}\psi\\ \qquad + (y + \varepsilon^*\sin(\psi))\cos(\psi)\\ x_3 = \psi, \quad x_4 = -\dfrac{\alpha}{\beta}u - x_1, \quad x_5 = v + \varepsilon^* r, \quad x_6 = r\end{cases}\tag{4}$$

and input transformations as

$$\begin{cases}w_1 = -\dfrac{\alpha}{\beta}\bar{\tau}_u^* + \dfrac{\beta}{\alpha}(x_1 + x_4) - x_2x_6 + \dfrac{1}{\beta}x_5x_6 - \dfrac{\gamma}{\beta}x_3x_6\\ \quad\ = -\dfrac{\alpha}{\beta m_{11}}\tau_u^* + \Xi\\ w_2 = \bar{\tau}_r^* = M^*\tau_r^* + \Delta_2\end{cases}\tag{5}$$

with $\varepsilon^* = \frac{m_{23}}{m_{22}}$, $\alpha = \frac{m_{11}}{m_{22}}$, $\beta = \frac{d_{22}}{m_{22}}$, $\gamma = \frac{d_{22}m_{23}}{m_{22}^2} - \frac{d_{23}}{m_{22}}$, $M^* = \frac{m_{22}}{m_{22}m_{33} - m_{23}m_{32}}$ and $\Xi = -\frac{\alpha}{\beta}\Delta_1 + \frac{\beta}{\alpha}(x_1 + x_4) + x_6\left(\frac{1}{\beta}x_5 - x_2 - \frac{\gamma}{\beta}x_3\right)$. Then, the ship model (1) can be rewritten into the following cascade form:

$$\Sigma_1: \begin{cases}\dot{x}_1 = -\dfrac{\beta}{\alpha}x_1 - \dfrac{\beta}{\alpha}x_4 + x_2x_6 - \dfrac{1}{\beta}x_5x_6 + \dfrac{\gamma}{\beta}x_3x_6\\ \dot{x}_5 = -\beta x_5 + \beta x_6(x_1 + x_4) + \gamma x_6\end{cases}\tag{6}$$

$$\Sigma_2: \dot{x}_2 = x_4x_6, \quad \dot{x}_3 = x_6, \quad \dot{x}_4 = w_1, \quad \dot{x}_6 = w_2. \tag{7}$$

Lemma 1 [5]: State transformations in (4) are invertible which implies that the stabilization problem of system (1) is successfully converted into the stabilization problem of the cascade system (6) and (7).

Lemma 2 [5]: Σ_1-subsystem is stable (or asymptotic stable) as long as Σ_2-subsystem is stable (or asymptotic stable).

Subsequently, to explore the control relationship between the considered underactuated ship and nonholonomic system in chained-form, the necessary state transformations are constructed as

$$\begin{cases} z_0 = x_4 \\ z_1 = x_2 - x_3 x_4 \\ z_2 = -x_3 \\ z_3 = -x_6 \end{cases} \Rightarrow \begin{cases} \dot{z}_0 = w_1 \\ \dot{z}_1 = z_2 w_1 \\ \dot{z}_2 = z_3 \\ \dot{z}_3 = -w_2 \end{cases} \tag{8}$$

from which, it concludes that the Σ_2-subsystem has been further transformed into a nonholonomic-like form (8). It is well-known that due to the triangular structure of (8), the control design is usually developed in two separate stages. Let the initial time $t_0 = 0$. The case $z_0(0) \neq 0$ is first considered and then the case $z_0(0) = 0$ is addressed.

Controller design under $z_0(0) \neq 0$.

Assume that $z_0(0) \neq 0$, we consider the candidate BLF as $V_0 = (1/2)\ln[b_0^2/(b_0^2 - z_0^2)]$ for z_0-subsystem, where $b_0 > 0$. Here, the control signal $w_1(z_0)$ is designed as

$$w_1 = -z_0 k \triangleq z_0 d_0, \quad k > 0. \tag{9}$$

Under which, it yields that

$$\dot{V}_0 = -kz_0^2/(b_0^2 - z_0^2) \leq -2kV_0 \tag{10}$$

where inequality $-z_0^2/(b_0^2 - z_0^2) \leq -\ln[b_0^2/(b_0^2 - z_0^2)]$ has been used.

Proposition 1: For the closed-loop z_0−subsystem with control law (9), if the initial condition $-b_0 < z_0(0) < b_0$ holds, then state $z_0(t)$ is bounded and $\lim_{t\to\infty} z_0(t) = 0$. At the same time, auxiliary state constraint $-b_0 < z_0(t) < b_0$ holds for all $t \in [0, \infty)$.

Proof: The proof of Proposition 1 can be referred to [12]. ■

Since $z_0(0) \neq 0$ has been assumed previously, consequently, w_1 specified by (9) can ensure that z_0 does not cross zero for any t. Since $\lim_{t\to\infty} z_0(t) = 0$ as well as $\lim_{t\to\infty} w_1(t) = 0$, $z = (z_1, z_2, z_3)$−subsystem is uncontrollable in the limit $w_1(t) = 0$. This obstacle can be remedied with the following discontinuous state scaling transformations:

$$y_1 = z_1/z_0, \quad y_2 = z_2, y_3 = z_3. \tag{11}$$

Applying control law (9) and state scaling (11) to system (8), z-subsystem can be converted into

$$\dot{y}_1 = d_0 y_2 - d_0 y_1, \quad \dot{y}_2 = y_3, \quad \dot{y}_3 = -w_2. \tag{12}$$

Furthermore, in order to handle state constraints, inspired by [13], the following SDF transformations are introduced as:

$$s_i = y_i/(\delta_i^2 - y_i^2), \quad \delta_i > 0, \quad i = 1,2,3 \tag{13}$$

which can dexterously convert the original state-constrained system (12) into an unconstrained new system, namely,

$$\dot{s}_1 = \mu_1(d_0 h_2 s_2 - d_0 y_1), \quad \dot{s}_2 = \mu_2 h_3 s_3, \quad \dot{s}_3 = -\mu_3 w_2 \tag{14}$$

where $h_i = \delta_i^2 - y_i^2$ $(2 \leq i \leq 3)$, $\mu_i = (\delta_i^2 + y_i^2)/(\delta_i^2 - y_i^2)^2$ $(1 \leq i \leq 3)$. Please refer to [13] for the properties of transformations in (13).

Let α_1 and α_2 be the virtual controllers in (14). In the sequel, the standard backstepping design is used to develop controller. The designed virtual control signals and the necessary inequalities in control design are summarized in Table 1, where $N_i > 0$ $(i = 2,3)$, $c_i > 0$ $(i = 1,2,3)$, $l_i = \frac{\alpha_{i-1}\dot{h}_i}{h_i^2} - \frac{\dot{\alpha}_{i-1}}{h_i}$ $(i = 2,3)$, $\dot{\alpha}_1 = \frac{\partial \alpha_1}{\partial \mu_1}\dot{\mu}_1 + \frac{\partial \alpha_1}{\partial e_1}\dot{e}_1 + \frac{\partial \alpha_1}{\partial y_1}\dot{y}_1$ and $\dot{\alpha}_2 = \frac{\partial \alpha_2}{\partial \mu_1}\dot{\mu}_1 + \frac{\partial \alpha_2}{\partial \mu_2}\dot{\mu}_2 + \frac{\partial \alpha_2}{\partial e_1}\dot{e}_1 + \frac{\partial \alpha_2}{\partial e_2}\dot{e}_2 + \frac{\partial \alpha_2}{\partial \dot{\alpha}_{2f}}\ddot{\alpha}_{2f} + \frac{\partial \alpha_2}{\partial h_2}\dot{h}_2$.

The entire candidate Lyapunov function can be chosen as

$$V_1 = \frac{1}{2}e_1^2 + \frac{1}{2}e_2^2 + \frac{1}{2}e_3^2 + \frac{1}{2}\chi_2^2 + \frac{1}{2}\chi_3^2. \tag{15}$$

Then, it can be deduced the following result:

$$\dot{V}_1 \leq -\sum_{j=1}^{3} c_j e_j^2 - \sum_{j=2}^{3} N_j^* \chi_j^2 + \sum_{j=2}^{3} l_j^2. \tag{16}$$

Proposition 2: If the initial conditions $-\delta_i < y_i(0) < \delta_i$ $(1 \leq i \leq 3)$ hold, the following control goals can can be achieved: 1) $-\delta_i < y_i(t) < \delta_i$ $(1 \leq i \leq 3)$ for any $t \geq 0$, 2) all closed-loop signals are bounded for $t \geq 0$.

Proof: The proof of Proposition 2 can refer to the proof of Proposition 2 in our previous work [12], and hence is omitted here. ■

Table 1. Virtual Control Errors, First-Order Filters, Virtual Controllers, Actual Controller and Inequalities in Control Design

Virtual control errors

$e_1 = s_1, \ e_i = s_i - \alpha_{if}, \ i = 2,3.$

First-order filters

$N_i \dot{\alpha}_{if} = \alpha_{i-1}/h_i - \alpha_{if}, i = 2,3$

$\chi_i = \alpha_{if} - \alpha_{i-1}/h_i, i = 2,3.$

Virtual controllers and actual controller

$\alpha_1 = \frac{1}{\mu_1 d_0}(-c_1 e_1 - e_1 d_0^2 \mu_1^2 + \mu_1 d_0 y_1)$

$\alpha_2 = \frac{1}{\mu_2}(-c_2 e_2 - e_2 \mu_2^2 + \dot{\alpha}_{2f} - e_1 \mu_1 d_0 h_2)$

$w_2 = \frac{1}{\mu_3}(c_3 e_3 - \dot{\alpha}_{3f} + e_2 h_3 \mu_2).$

Inequalities in control design

$e_1 \mu_1 d_0 h_2 \chi_2 \leq d_0^2 \mu_1^2 e_1^2 + \frac{1}{4}h_2^2 \chi_2^2$

$e_2 \mu_2 h_3 \chi_3 \leq e_2^2 \mu_2^2 + \frac{1}{4}h_3^2 \chi_3^2$

$\chi_i \dot{\chi}_i = -\frac{\chi_i^2}{N_i} + \chi_i l_i \leq (\frac{1}{4} - \frac{1}{N_i})\chi_i^2 + l_i^2, \ i = 2,3$

$N_i^* \leq \frac{1}{N_i} - \frac{1}{4}h_i^2 - \frac{1}{4}, \ i = 2,3.$

Switching control when $z_0(0) = 0$.

Next, the control design of w_1 and w_2 will be discussed in the case of $z_0(0) = 0$ since transformation (11) can not be carried out if $z_0(0) = 0$. When $z_0(0) = 0$, the actual control w_1 is chosen as

$$w_1 = -k_0 z_0 + w_{1c}\sqrt{b_0^2 - z_0^2} \tag{17}$$

where constants $k_0 > 0$ and $w_{1c} > 0$. Considering the same BLF V_0 presented above, one has

$$\dot{V}_0 \leq -(k_0 - 1/2)z_0^2/(b_0^2 - z_0^2) + w_{1c}^2/2 \tag{18}$$

where positive constants k_0 and w_{1c} are chosen to satisfy $k_0 > \frac{1}{2}$ and $w_{1c}/\sqrt{2k_0 - 1} < 1$. According to (18), $V_0 \in \mathcal{L}_\infty$. Meanwhile, it can be seen that $\dot{V}_0$ is negative once $|z_0(t)| \geq (w_{1c}b_0)/\sqrt{2k_0 - 1}$. Hence, as long as $|z_0(0)| < b_0$, $z_0(t)$ is bounded, thus, $|z_0(t)| < b_0$ for any $t \geq 0$. Under (17), the z_0-subsystem is described as

$$\dot{z}_0 = -z_0 k_0 + w_{1c}\sqrt{b_0^2 - z_0^2}. \tag{19}$$

Therefore, it can be concluded that for any given finite time t_f such that $w_1(t) > 0$ $(0 \leq t \leq t_f)$, state $z_0(t)$ keeps positive and does not escape. On time interval $[0, t_f]$, under w_1 defined by (17) instead of (9), we can apply the backstepping to design feedback control $w_2^*(z_0, z_1, z_2, z_3)$ which can ensure the desired state constraints. Since $z_0(t_f) \neq 0$, state scaling transformation (11) can be used, therefore, input w_1 can be switched into (9) at time $t = t_f$.

Proposition 3: Consider $\bar{z} = (z_0, z_1, z_2, z_3)$−system specified in (8), if the following switching control scheme is actuated to it in such a way: 1) when $z_0(0) \neq 0$, $w_1 = (9)$ and $w_2 = (1/\mu_3)(c_3 e_3 - \dot{\alpha}_{3f} + e_2 h_3 \mu_2)$; 2) when $z_0(0) = 0$, $w_1 = (17) \to w_1 = (9)_{t=t_f}$ and $w_2 = w_2^*(z_0, z_1, z_2, z_3) \to w_2 = (1/\mu_3)(c_3 e_3 - \dot{\alpha}_{3f} + e_2 h_3 \mu_2)_{t=t_f}$. Then, system (8) is bounded while the full-state constraints $|z_0(t)| < b_0$, $|z_1(t)| < \delta_1 b_0$, $|z_2(t)| < \delta_2$, and $|z_3(t)| < \delta_3$ are not violated by choosing appropriate initial conditions.

The original state constrains analysis and main results.

From state transformations in (8), Propositions 1−3, the following state constraints can be summarized as:

$$\begin{cases} |z_0(t)| < b_0 \\ |z_1(t)| < \delta_1 b_0 \\ |z_2(t)| < \delta_2 \\ |z_3(t)| < \delta_3 \end{cases} \Rightarrow \begin{cases} |x_2(t)| = |z_1 + x_3 x_4| < b_0(\delta_1 + \delta_2) \\ |x_3(t)| < \delta_2 \\ |x_4(t)| < b_0 \\ |x_6(t)| < \delta_3. \end{cases} \tag{20}$$

Next, to analyze the constraints on the original system states $x(t)$, $y(t)$, $\psi(t)$, $u(t)$, $v(t)$, and $r(t)$, we first select the candidate Lyapunov function for Σ_1-subsystem in (6) as $V_2 = (1/2)\beta^2 x_1^2 + (1/2)x_5^2$. Computing its time derivative results in

$$\dot{V}_2 = -\frac{\beta^3}{\alpha}x_1^2 - \frac{\beta^3}{\alpha}x_1x_4 + \beta^2 x_1x_2x_6 + \beta\gamma x_1x_3x_6 - \beta x_5^2 + \beta x_4x_5x_6 + \gamma x_5x_6. \quad (21)$$

Define $\sigma_1 = 2\min\{\frac{\beta^3}{\alpha},\beta\}/\max\{\beta^2,1\}$ and $\sigma_2(t) = \sqrt{2}\sqrt{\max\left\{\frac{2}{\beta^2},2\right\}}\times \max\left\{\beta\left(\frac{\beta^2}{\alpha}|x_4(t)|+\beta|x_2(t)x_6(t)|+\gamma|x_3(t)x_6(t)|\right),\beta|x_4(t)x_6(t)|+\gamma|x_6(t)|\right\}$. Due to (20), the upper bound of σ_2 can be defined as

$$\sigma_2(t) \le \bar{\sigma} = \sqrt{2}\sqrt{\max\left\{\frac{2}{\beta^2},2\right\}}\max\left\{\beta\left(\frac{\beta^2}{\alpha}b_0+\gamma\delta_2\delta_3 + \beta(\delta_1+\delta_2)b_0\delta_3\right),\beta b_0\delta_3+\gamma\delta_3\right\}. \quad (22)$$

With inequality $|a|+|b| \le \sqrt{2(a^2+b^2)}$ $(a,b\in\mathbb{R})$ in mind, (21) can be rewritten as

$$\dot{V}_2 \le -\sigma_1 V_2 + \sigma_2(t)\sqrt{V_2} \le -\sigma_1 V_2 + \bar{\sigma}\sqrt{V_2}. \quad (23)$$

By defining $W = \sqrt{V_2}$, from (23) it can be deduced that $\dot{W} \le -\frac{\sigma_1}{2}W + \frac{1}{2}\bar{\sigma}$. Hence, it can be computed that $W \le W(0) + \frac{\bar{\sigma}}{\sigma_1}$. Reviewing the definition of V_2, we can claim that

$$|x_1(t)| \le B_0, |x_5(t)| \le B_1 \quad (24)$$

where $B_0 = \frac{\sqrt{2}}{\beta}\left(W(0)+\frac{\bar{\sigma}}{\sigma_1}\right)$ and $B_1 = \sqrt{2}\left(W(0)+\frac{\bar{\sigma}}{\sigma_1}\right)$. Therefore, under (20) and state transformation (4), the state constraints on the original system states $x(t)$, $y(t)$, $\psi(t)$, $u(t)$, $v(t)$, and $r(t)$, can be described as

$$\begin{aligned}
|x(t)| &\le \sqrt{x^2+y^2} = x\cos(\psi)+y\sin(\psi) \\
&= x_1 - \varepsilon^*(1-\cos(\psi)) \le |x_1| \le B_0 \\
|y(t)| &\le \sqrt{x^2+y^2} = x\cos(\psi)+y\sin(\psi) \\
&= x_1 - \varepsilon^*(1-\cos(\psi)) \le |x_1| \le B_0 \\
|\psi(t)| &= |x_3| \le \delta_2, |r(t)| = |x_6| \le \delta_3 \\
|u(t)| &= |\frac{\beta}{\alpha}(x_1+x_4)| \le \frac{\beta}{\alpha}(B_0+b_0) \\
|v(t)| &= |x_5 - \varepsilon^* r| \le |x_5| + |\varepsilon^* r| \le B_1 + \varepsilon^*\delta_3.
\end{aligned} \quad (25)$$

Therefore, in view of (25), to realize the desired state constraints $|x(t)|<k_x$, $|y(t)|<k_y$, $|\psi(t)|<k_\psi$, $|u(t)|<k_u$, $|v(t)|<k_v$, $|r(t)|<k_r$, the introduced control parameters b_0 and δ_i $(1\le i\le 3)$ should comply with the following relationships:

$$\begin{aligned}
&B_0 < k_x, \quad B_0 < k_y, \quad \delta_2 < k_\psi, \quad \frac{\beta}{\alpha}(B_0+b_0) < k_u \\
&B_1 + \varepsilon^*\delta_3 < k_v, \quad \delta_3 < k_r.
\end{aligned} \quad (26)$$

Theorem 1: Consider the underactuated surface ship (1), if the stabilization controllers are applied in the following way: 1) when $z_0(0)\neq 0$, $w_1 = (9)$ and $w_2 = (1/\mu_3)(c_3e_3 - \dot{\alpha}_{3f} + e_2h_3\mu_2)$; 2) when $z_0(0)=0$, $w_1 = (17) \to w_1 = (9)_{t=t_f}$ and $w_2 = w_2^*(z_0,z_1,z_2,z_3) \to w_2 = (1/\mu_3)(c_3e_3 - \dot{\alpha}_{3f} + e_2h_3\mu_2)_{t=t_f}$, and the auxiliary control parameters b_0 and δ_i $(1\le i\le 3)$ are chosen to satisfy the relationship (26), then the resulting closed-loop system is bounded and the prespecified state constraints are not violated.

Simulation results: The simulation ship is the Cybership II in [5]. A difference is that the non-diagonal and nonzero-constant terms in **M** and **D** are replaced with 0.001 and −0.001, respectively. To comply with the relationship (26), the designed the control parameters are chosen as $k=10$, $c_1=10$, $c_2=10$, $c_3=30$, $\delta_1=0.32$, $\delta_2=1$, $\delta_3=0.3$, $N_2=11$, and $N_3=10$. The desired constraint boundaries are picked as $k_x=3.45$, $k_y=3.45$, $k_\psi=1$, $k_u=0.39$, $k_v=0.3$, and $k_r=0.3$. In simulation, system initial conditions are configured as $x(0)=2.32$ m, $y(0)=1.49$ m, $\psi(0)=0.57$ rad, $u(0)=0$ m/s, $v(0)=0$ m/s, $r(0)=0$ rad/s and filter initial states are chosen as $\alpha_{2f}(0)=0$ and $\alpha_{3f}(0)=0$. According to the Fig. 1, all system states are bounded and quickly converge to zero, and satisfy the given state constraints.

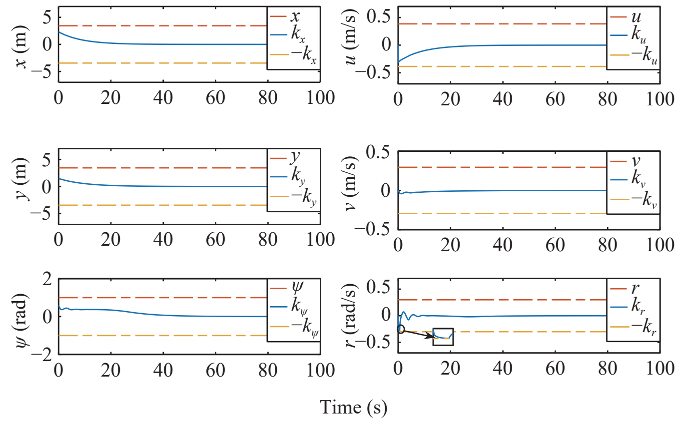

Fig. 1. The responses of the system states.

Acknowledgment: This work was supported by the National Natural Science Foundation of China (62173207, 62073187, 62073189) and the Major Scientific and Technological Innovation Project in Shandong Province (2019JZZY011111).

References

[1] Z. H. Peng, J. Wang, D. Wang, and Q.-L. Han, "An overview of recent advances in coordinated control of multiple autonomous surface vehicles," *IEEE Trans. Industrial Informatics*, vol. 17, no. 2, pp. 732–745, 2021.

[2] Y. Q. Wu, Z. C. Zhang, and N. Xiao, "Global tracking controller for underactuated ship via switching design," *J. Dynamic Syst., Measurement, and Control*, vol. 136, no. 9, p. 054506, 2014.

[3] B. L. Ma and W. J. Xie, "Global asymptotic trajectory tracking and point stabilization of asymmetric underactuated ships with non-diagonal inertia/damping matrices," *Int. J. Advanced Robotic Systems*, vol. 10, pp. 1–9, 2013.

[4] K. D. Do, "Robust adaptive tracking control of underactuated ODINs under stochastic sea loads," *Robotics and Autonomous Systems*, vol. 72, pp. 152–163, 2015.

[5] Z. C. Zhang and Y. Q. Wu, "Further results on global stabilisation and tracking control for underactuated surface vessels with non-diagonal inertia and damping matrices," *Int. J. Control*, vol. 88, no. 9, pp. 1679–1692, 2015.

[6] G. Q. Zhang, S. J. Chu, X. Jin, and W. D. Zhang, "Global composite neural learning fault-tolerant control for underactuated vehicles with event-triggered input," *IEEE Trans. Cybernetics*, vol. 51, no. 5, pp. 2327–2338, 2021.

[7] Z. P. Dong, L. Wan, Y. M. Li, T. Liu, and G. C. Zhang, "Trajectory tracking control of underactuated USV based on modified backstepping approach," *Int. J. Naval Architecture and Ocean Engineering*, vol. 7, no. 5, pp. 817–832, 2015.

[8] H. Katayama and H. Aoki, "Straight-line trajectory tracking control for sampled-data underactuated ships," *IEEE Trans. Control Systems Technology*, vol. 22, no. 4, pp. 1638–1645, 2014.

[9] Y. Liu, H. Y. Li, Z. Y. Zuo, X. D. Li, and R. Q. Lu, "An overview of finite/fixed-time control and its application in engineering systems," *IEEE/CAA J. Autom. Sinica*, 2022. DOI: 10.1109/JAS.2022.105413.

[10] J. X. Zhang and G. H. Yang, "Fault-tolerant fixed-time trajectory tracking control of autonomous surface vessels with specified accuracy," *IEEE Trans. Industrial Electronics*, vol. 67, no. 6, pp. 4889–4899, 2020.

[11] F. Mazenc, K. Y. Pettersen, and H. Nijmeijer, "Global uniform asymptotical stabilization of an underactuated surface vessel," *IEEE Trans. Automatic Control*, vol. 47, pp. 1759–1762, 2002.

[12] Z. C. Zhang, S. M. Zhang, and Y. Q. Wu, "New stabilization controller of state-constrained nonholonomic systems with disturbances: Theory and experiment," *IEEE Trans. Industrial Electronics*, vol. 70, no. 1, pp. 669–677, 2023.

[13] Y. Cao, Y. D. Song, and C. Y. Wen, "Practical tracking control of perturbed uncertain nonaffine systems with full state constraints," *Automatica*, vol. 110, p. 108608, 2019.